Microwave Spectrum of 1-Butene Oxide

S. O. Ljunggren and P. J. Mjöberg

Department of Physical Chemistry, Royal Institute of Technology, S-100 44 Stockholm, Sweden

and

J. E. Bäckvall

Department of Organic Chemistry, Royal Institute of Technology, S-100 44 Stockholm, Sweden

Z. Naturforsch. **33 a**, 1312–1322 (1978); received July 18, 1978

The microwave spectrum of 1-butene oxide in the gas phase has been studied in the frequency region 18.0–39.0 GHz. The spectrum observed arose from a rotamer with a dihedral H–C_2–C_3–C_4 angle of 59° ± 1°. In addition to several Q-branch progressions the spectrum contained several long perpendicular ^RP and ^PR progressions. However, of the ground state lines, only the intermediate ^PR transitions showed internal rotation splittings that could be resolved to yield a barrier height of 3.02 kcal mol^{-1}. The value derived from the line splittings of the first excited methyl torsional state was slightly higher (3.17 kcal mol^{-1}) but must be regarded as being less reliable. The components of the dipole moment, the rotational constants, and the quartic and sextic centrifugal distortion coefficients for the ground state and three vibrationally excited states were determined.

Introduction

The preferred conformation of 1,2-disubstituted ethanes and analogous ethane fragments often differ from what would be predicted on steric grounds [1]. On the basis of steric bulk and size these molecules would be expected to be more stable in an *anti* rather than in a *gauche* conformation, which is true for a large number of molecules. However, when electron pairs or polar bonds are present there is usually a strong preference for the *gauche* conformation. Examples of this include 2-haloethanols [2], propyl halides [3], 1,2-dimethoxyethane [4], and many other compounds.

Microwave studies have been performed on cyclopropyl methyl ether [5] and on epifluorohydrin [6], molecules with a structure similar to that of 1-butene oxide. As expected, epifluorohydrin prefers a conformation that is *gauche* with respect to the oxygen atom, while the cyclopropyl methyl ether molecule may assume two equivalent conformations.

The purpose of the present study was to determine the preferred conformation of 1-butene oxide and to study the barrier to internal rotation of the methyl group in this molecule.

Experimental

The sample of 1-butene oxide was obtained from Fluka AG and was further purified by distillation.

Microwave spectra were recorded using a Hewlett-Packard Model 8460 A spectrometer equipped with a phase-stabilised source oscillator and with a Stark cell modulation frequency of 33.33 kHz. The measurements were carried out at −20 °C (253 K) in the frequency region 18.0–39.0 GHz with sample pressures of 9 to 55 mTorr (1.2 to 7.3 Pa).

Microwave Spectrum

The 1-butene oxide molecule is a prolate asymmetric rotor with $\varkappa = -0.936$ and with the main component of the dipole moment along the b axis.

The strongest lines in the spectrum are b-type Q-branch progressions of the type

$$J_{K,J-K} \leftarrow J_{K-1,J-K+1}$$

with $K = 1, 2$ or 3 (Figure 1). These lines were easily assigned using current methods. In addition to the ground state transitions, two other complete sets of Q-branch transitions with the approximate relative intensities 0.56 and 0.31 (in relation to the ground state) at −20 °C could be assigned to the first and second excited states of the heavy atom torsion, respectively. Another set of Q-branch transitions with a relative intensity of 0.28 was observed rather close to the ground state lines. These lines appeared to be single during a rapid scan (1 MHz s^{-1}) at 55 mTorr (7.3 Pa) but were found to be split upon slow scanning at 9 mTorr (1.2 Pa). The splittings ranged from 0.5 to 1.1 MHz

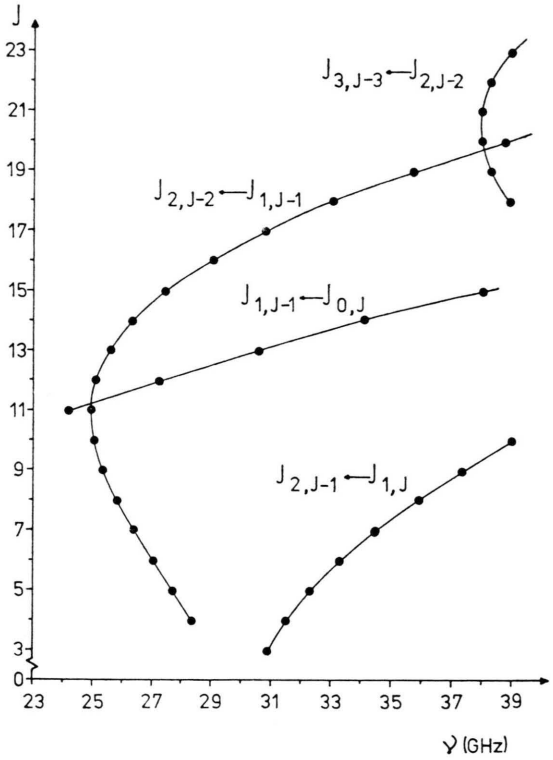

Fig. 1. Fortrat diagram of Q-branch transitions for 1-butene oxide.

and the lines were therefore assigned to the first excited state of the methyl torsion. It should be pointed out that no rotational splitting was observed in the ground state Q-lines.

In addition to the Q-branch progressions the spectrum contains several progressions of strong perpendicular ${}^{P}R$ ($\Delta J = 1$, $\Delta K_{-1} = -1$) and ${}^{R}P$ ($\Delta J = -1$, $\Delta K_{-1} = 1$) transitions. The ${}^{R}P$ transitions occur in nearly degenerate pairs of

$$(J-1)_{K+1,J-K-1} \leftarrow J_{K,J-K}$$

and

$$(J-1)_{K+1,J-K-2} \leftarrow J_{K,J-K+1}$$

with $J = 3K-3$, $3K-2$, $3K-1$, $3K$ and $3K+1$, for K values between 6 and 19. For convenience, these degenerate pairs will be denoted

$$(J-1)_{K+1} \leftarrow J_K\,.$$

As shown in Fig. 2, the transition frequencies for each of these families is an almost linear function of K. This is also true, with no noticeable deviation from linearity at all, for the so-called $\bar{\tau}$ families, where $\bar{\tau}$ is the mean value of τ ($= K_{-1} - K_1$) for the initial and final states of a transition. This type of relationship is typical of high-K perpendicular transitions of a near-prolate or near-oblate rotor, as was shown by Herschbach and Swalen [7] in connection with the microwave spectrum of propylene oxide. Starting from the perturbational expression for the energy levels of an almost symmetric rotor

$$E_{JK} = (1/2)(B+C)J(J+1) + [A - (1/2)(B+C)] \times (K_{-1}^2 + c_1 b + c_2 b^2 + \cdots)\,,$$

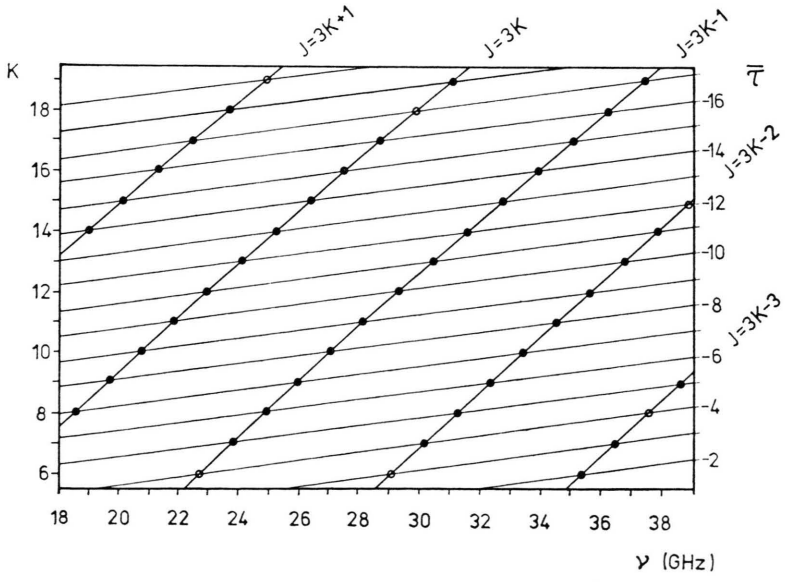

Fig. 2. Pattern of high-K, ${}^{P}P$ transitions of the type $(J-1)_{K+1} \leftarrow J_K$. The empty circles represent transitions which could not be measured due to overlapping with other spectral lines.

where $b=(C-B)/(2A-B-C)$ is the Wang asymmetry parameter, these investigators showed that the frequency difference between successive members of a $\bar{\tau}$ family is nearly constant at high K values.

A similar derivation for a "family" with $J=3K+n$ yields the following expression for the frequency of a $(J-1)_{K+1} \leftarrow J_K$, ${}^RP$ transition

$$\begin{aligned} \nu = {} & 2[A-2(B+C)]K \\ & + [A-(B+C)(n+(1/2))] \\ & + [A-(1/2)(B+C)](b^2 \Delta c_2 + \cdots), \end{aligned}$$

where we have omitted Δc_1, which is zero for K values larger than 1. It can be seen that if $A-2(B+C)$ is small (580.23 MHz for 1-butene oxide), numerous perpendicular transitions with different K values will appear in the spectrum.

Most of the R-lines are ${}^PR$ transitions which appear in pairs of the sort

$$J_{K,J-K} \leftarrow (J-1)_{K+1,J-K-1} \quad \text{and}$$
$$J_{K,J-K+1} \leftarrow (J-1)_{K+1,J-K-2}\,.$$

These pairs also become nearly degenerate for K values equal to or greater than 10 and exhibit a pattern similar to that of the ${}^RP$ transitions but with an opposite dependence on K (Figure 3).

In this type of spectrum the assignment of R- and P-branch transitions is sometimes difficult because of the low intensity of the low J transitions and the considerable displacement of the high J transitions by centrifugal distortion. The following method facilitated the assignment.

The frequency of an R-branch transition can be written as follows:

$$\nu = (A+C)(J+1) + [(A-C)/2]\,\Delta E(\varkappa)\,,$$

where $E(\varkappa)$ is the reduced energy. If the Q-lines have already been assigned, then $A-C$ and $\varkappa$ are known. Thus, the last term in the expression for ν can be regarded as a constant. From the assumed structure or by other means the value of $A+C$ is then estimated ($(A+C)_{\text{est}}$). The estimated frequency thus becomes

$$\nu_{\text{est}} = (A+C)_{\text{est}}(J+1) + \text{const.}$$

However, the true frequency is

$$\nu_{\text{true}} = (A+C)_{\text{true}}(J+1) + \text{const.}$$

Thus,

$$\begin{aligned} & \nu_{\text{true}} - \nu_{\text{est}} \\ & \quad = (J+1)\,[(A+C)_{\text{true}} - (A+C)_{\text{est}}] \end{aligned}$$

or

$$\begin{aligned} \delta\nu &= (J+1)\,\delta(A+C) \\ &= 2(J+1)\,\delta C \end{aligned}$$

which means that

$$\delta\nu/(J+1) = \delta(A+C)\,.$$

By calculating $\delta\nu/(J+1)$ for several different lines in the neighbourhood of ν_{est} for two or more R transitions the assignment is easily completed, since $\delta\nu/(J+1)$ should be independent of J for the true lines. The high-J, R- or P-branch transitions can then be determined by successively adjusting the centrifugal distortion coefficients.

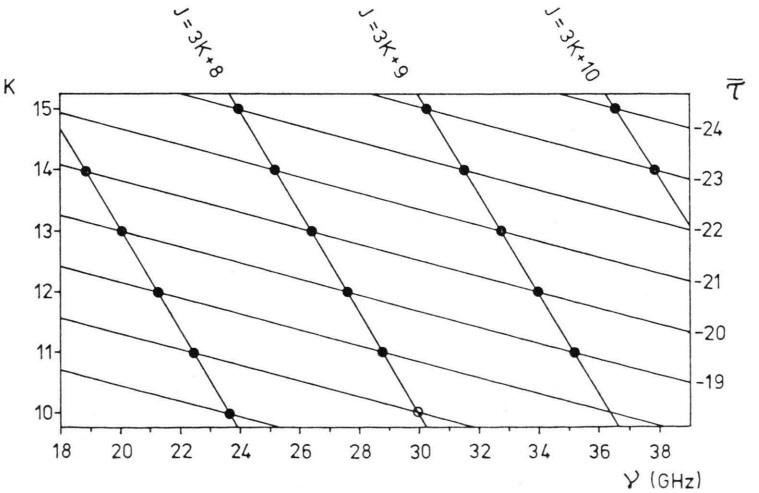

Fig. 3. Pattern of high-K, ${}^PR$ transitions of the type $J_K \leftarrow (J-1)_{K+1}$.

Table 1. Selected transitions for the vibrational ground state of 1-butene oxide.

Transition	Observed frequency (MHz)	Obs.-calc. frequency (MHz)	Centrifugal distortion Total (MHz)	Centrifugal distortion Sextic (MHz)
[b]*Q* type				
$3_{22} \leftarrow 3_{13}$	30802.84	−0.03	− 0.34	0.00
$4_{22} \leftarrow 4_{13}$	28343.51	0.04	0.13	0.00
$4_{23} \leftarrow 4_{14}$	31459.29	−0.04	− 0.19	0.00
$5_{24} \leftarrow 5_{15}$	32284.00	0.02	− 0.07	0.00
$7_{25} \leftarrow 7_{16}$	26387.43	−0.03	1.59	0.00
$9_{18} \leftarrow 9_{09}$	19022.52	−0.01	− 3.14	0.00
$11_{1,10} \leftarrow 11_{0,11}$	24154.70	0.02	− 7.68	0.00
$15_{2,13} \leftarrow 15_{1,14}$	27427.99	−0.01	− 6.16	− 0.02
$18_{3,15} \leftarrow 18_{2,16}$	38933.53	−0.02	22.49	− 0.09
$21_{3,18} \leftarrow 21_{2,19}$	37909.49	0.00	10.98	− 0.13
$23_{3,20} \leftarrow 23_{2,21}$	38976.29	0.01	−11.51	− 0.15
[b]*R* type				
$2_{12} \leftarrow 1_{01}$	21940.52	0.02	0.00	0.00
$3_{13} \leftarrow 2_{02}$	27699.83	0.01	− 0.02	0.00
$4_{14} \leftarrow 3_{03}$	33310.46	0.02	− 0.07	0.00
$5_{05} \leftarrow 4_{14}$	22627.56	0.01	− 1.08	0.00
$7_{07} \leftarrow 6_{16}$	36282.86	0.03	− 2.83	0.00
$9_{18} \leftarrow 8_{27}$	33169.36	0.05	− 8.48	0.00
$11_{29} \leftarrow 10_{38}$	22706.72	0.02	−14.88	0.00
$15_{2,14} \leftarrow 14_{3,11}$	38339.46	0.09	−16.63	0.00
$20_{4,16} \leftarrow 19_{5,15}$	37804.27	0.03	−77.78	0.06
$20_{4,17} \leftarrow 19_{5,14}$	36747.51	−0.04	−69.40	0.06
$23_{5,18} \leftarrow 22_{6,17}$	36045.76	−0.05	−108.12	0.13
$23_{5,19} \leftarrow 22_{6,16}$	35828.38	−0.05	−105.18	0.13
$37_{10,27} \leftarrow 36_{11,26}$	23561.81	−0.04	−370.75	1.21
$37_{10,28} \leftarrow 36_{11,25}$	23561.81	−0.02	−370.76	1.20
$40_{11,29} \leftarrow 39_{12,28}$	22387.90	−0.04	−459.44	1.76
$40_{11\ 30} \leftarrow 39_{12,27}$	22387.90	−0.04	−459.44	1.76
$45_{12,33} \leftarrow 44_{13,32}$	33904,95	0.14	−685.22	3.25
$45_{12,34} \leftarrow 44_{13,31}$	33904.95	0.14	−685.22	3.25
$50_{14,36} \leftarrow 49_{15,35}$	25124.43	−0.01	−883.64	5.32
$50_{14,37} \leftarrow 49_{15,34}$	25124.43	−0.01	−883.64	5.32
$55_{15,40} \leftarrow 54_{16,39}$	36517.81	0.00	−1224.41	8.75
$55_{15,41} \leftarrow 54_{16,38}$	36517.81	0.00	−1224.41	8.75
[b]*P* type				
$17_{89} \leftarrow 18_{7,12}$	36435.73	0.00	− 3.13	− 0.01
$17_{8,10} \leftarrow 18_{7,11}$	36435.73	0.01	− 3.13	− 0.02
$21_{9,12} \leftarrow 22_{8,15}$	31223.35	−0.01	19.95	− 0.06
$21_{9,13} \leftarrow 22_{8,14}$	31223.35	−0.01	19.95	− 0.06
$23_{9,14} \leftarrow 24_{8,17}$	18604.24	0.00	55.28	− 0.10
$23_{9,15} \leftarrow 24_{8,16}$	18604.24	0.01	55.28	− 0.10
$23_{10,13} \leftarrow 24_{9,16}$	38608.53	−0.06	16.23	− 0.08
$23_{10,14} \leftarrow 24_{9,15}$	38608.53	−0.06	16.23	− 0.08
$25_{10,15} \leftarrow 26_{9,18}$	26009.22	0.00	58.16	− 0.14
$25_{10,16} \leftarrow 26_{9,17}$	26009.22	0.00	58.16	− 0.14
$30_{12,18} \leftarrow 31_{11,21}$	34505.38	0.00	87.88	− 0.33
$30_{12,19} \leftarrow 31_{11,20}$	34505.38	0.00	87.88	− 0.33
$40_{15,25} \leftarrow 41_{14,28}$	31570.05	−0.02	277.70	− 1.46
$40_{15\ 26} \leftarrow 41_{14,27}$	31570.05	−0.02	277.70	− 1.46
$50_{18,32} \leftarrow 51_{17,35}$	28766.00	−0.01	612.92	− 4.61
$50_{18,33} \leftarrow 51_{17.34}$	28766.00	−0.01	612.92	− 4.61
$54_{19,35} \leftarrow 55_{18,38}$	23701.92	0.00	828.52	− 6.99
$54_{19,36} \leftarrow 55_{18,37}$	23701.92	0.00	828.52	− 6.99

The P-, Q- and R-lines of the ground state and the first excited heavy atom torsional state could easily be fitted to a rigid rotor spectrum using the Watson quartic and sextic centrifugal distortion correction terms [8]. In addition, the centrifugal distortion coefficients were found to be very nearly equal for the two states.

In contrast, the R- and P-lines of the second excited heavy atom torsional state could not be fitted to a rigid rotor spectrum, which indicates that this vibrational state must be perturbed by some other vibrational mode.

No attempt was made to assign the R- and P-lines of the first excited methyl torsional mode since these lines are expected to be strongly split and of low intensity and thus difficult to distinguish from other vibrational satellites.

Table 1 lists selected ground state transitions and their centrifugal distortion displacements. In order to deal with the centrifugal distortion the matrix of the Watson reduced Hamiltonian [8] with quartic and sextic terms was set up in a basis of symmetric top wave functions and diagonalized exactly. (The computer program used was the ASFIT program of A. Bauder, Swiss Federal Institute of Technology, Zurich expanded by the authors to include the sextic centrifugal distortion terms.) To obtain a satisfactory fit it was necessary to include those sextic terms (H_J, H_{JK}, H_{KJ}, and H_K) which are diagonal in K. The sextic part of the

Table 2. Rotational and centrifugal distortion constants for 1-butene oxide in the ground state and the first excited state of the heavy atom torsion (T1).

	Ground state		T1	
Number of transitions	158		97	
σ (MHz)[a]	0.036		0.029	
A (MHz)	13063.3939	± 0.0032[b]	13051.2757	± 0.0040
B (MHz)	3282.54701	± 0.00080	3276.4977	± 0.0010
C (MHz)	2959.03650	± 0.00085	2957.2385	± 0.0010
Δ_J (kHz)	1.6594	± 0.0034	1.6377	± 0.0038
Δ_{JK} (kHz)	−10.400	± 0.035	−10.217	± 0.040
Δ_K (kHz)	42.319	± 0.019	42.279	± 0.020
δ_J (kHz)	0.29824	± 0.00045	0.29422	± 0.00045
δ_K (kHz)	3.106	± 0.048	3.121	± 0.049
H_J (Hz)	−0.0039	± 0.0038	−0.0018	± 0.0039
H_{JK} (Hz)	−0.168	± 0.081	−0.122	± 0.083
H_{KJ} (Hz)	0.063	± 0.021	0.056	± 0.032
H_K (Hz)	−0.29	± 0.13	−0.16	± 0.14

[a] σ is the standard deviation of the fit.
[b] The uncertainty indicated is one standard deviation.

Table 3. Molecular constants for 1-butene oxide in the second excited state of the heavy atom torsion (T 2) and the A and E sublevels of the first excited state of the methyl torsion (M 1).

	T 2	M 1 A	M 1 E
Number of transitions	24[a]	7[a]	7[a]
σ (MHz)[b]	0.034	0.0087	0.0048
$A-C$ (MHz)	10077.410 ± 0.016[c]	10098.515 ± 0.022	10098.809 ± 0.012
$\varkappa$	−0.9371815 ± 0.0000064	−0.9361546 ± 0.0000089	−0.9361546 ± 0.0000048
Δ_J (kHz)	1.6594*[d]	1.6594*	1.6594*
Δ_{JK} (kHz)	−10.09 ± 0.12	−11.12 ± 0.24	−10.88 ± 0.13
Δ_K (kHz)	54.4 ± 4.5	42.319*	42.319*
δ_J (kHz)	0.31484 ± 0.00095	0.2769 ± 0.0018	0.27268 ± 0.00097
δ_K (kHz)	4.676 ± 0.098	2.49 ± 0.26	2.51 ± 0.14
H_J (Hz)	− 0.0039*	− 0.0039*	− 0.0039*
H_{JK} (Hz)	− 0.168*	− 0.168*	− 0.168*
H_{KJ} (Hz)	0.063*	0.063*	0.063*
H_K (Hz)	− 0.29*	− 0.29*	−0.29*

[a] All transitions involved belonged to the Q branch type of lines.
[b] σ is the standard deviation of the fit.
[c] The uncertainty indicated is one standard deviation.
[d] The coefficients marked with an asterix were held fixed at their ground state values during the fit.

centrifugal distortion was not large enough to allow the non-diagonal sextic terms (h_J, h_{JK}, and h_K) to be determined. However, as has been discussed by Steenbeckeliers and Bellet [9], for large K values the non-diagonal terms are negligible compared to the diagonal ones.

The spectroscopic constants calculated in this way for the ground state and the first excited heavy atom torsional state are listed in Table 2 and those for the second excited heavy atom torsional state and for the first excited methyl torsional state are shown in Table 3. In the last two cases only Q-lines have been measured. For this reason and because of the rather small number of observed transitions the Δ_J quartic coefficient and the sextic coefficients were held fixed at their ground state values during the least squares fit.

Finally, it should be pointed out that when using a direct diagonalization procedure with the centrifugal distortion terms included in the Hamiltonian the near degeneracy of the high-K levels is of no concern and will not require use of the symmetric-rotor centrifugal-distortion theory.

Internal Rotation

Using the principal axis method (PAM) of Herschbach [10] with four terms in the perturbation series expansion, the splittings of the lines belonging to the first excited state of the methyl torsion were found to correspond to a barrier height of 3.166 kcal mol^{-1} or $s = 88.15$. From the intensities of these lines relative to those of the ground state lines the approximate value $s = 89.9$ was calculated using the formula

$$E_{1A} - E_{0A} = 2.25\, F\,(b_{10} - b_{00})/c\,,$$

where F is the reciprocal of the reduced moment of inertia for the internal motion, $b_{v\sigma}$ are the eigenvalues of Mathieu's equation, and c is the velocity of light. The general agreement is obvious in spite of the error involved in the measurement of relative intensities. Table 4 shows the splittings of the Q-lines of the first excited methyl torsional state. Table 5 shows the internal rotation parameters used. The molecular constants used were the same as for the ground state and the accuracy of measurement did not warrant any attempt to adjust these parameters to obtain a better fit.

Calculations with the PAM revealed further that the expected splittings of the ground state Q-lines with $s \geqq 80$ (all with $K \leqq 3$) and those of ground state ^PR transitions for which $K \leqq 5$ are too small to be detectable with the resolution obtained (i.e., these splittings are less than 0.1 MHz).

For the $_RP$ transitions with $K \geqq 7$ the asymmetry splitting is almost negligible. As shown by Herschbach and Swalen [7], the line structure in this case consists of two E lines and a single A line of twice the intensity. This E-level splitting is due to the

Table 4. Transition frequencies (MHz) and internal rotation splittings (MHz) of the first excited methyl torsional state of 1-butene oxide.

Transition	A state (obs.)	E state (obs.)	$E - A$ (obs.)	$E - A$ (calc.[a])	$E - A$ (calc.[b])
$9_{18} \leftarrow 9_{09}$	18981.18	18981.77	0.59	0.60	0.60
$10_{19} \leftarrow 10_{0,10}$	21370.68	21371.36	0.68	0.69	0.69
$10_{28} \leftarrow 10_{19}$	25007.95	25008.60	0.65	0.64	0.64
$11_{1,10} \leftarrow 11_{0,11}$	24092.82	24093.62	0.80	0.79	0.78
$12_{2,10} \leftarrow 12_{1,11}$	25067.54	25068.20	0.66	0.66	0.66
$13_{2,11} \leftarrow 13_{1,12}$	25512.12	25512.80	0.68	0.69	0.69
$14_{2,12} \leftarrow 14_{1,13}$	26275.75	26276.49	0.74	0.74	0.73

[a] Calculated by the principal axis method with four perturbation terms [10].
[b] Calculated using the general IAM program of R. C. Woods, III [11]. The calculated splittings correspond to $s = 88.15$.

Table 5. Internal rotation parameters of 1-butene oxide.

Parameter	Ground state	First excited methyl torsional state
I_α (a.m.u. Å^2)	3.20[a]	3.20[a]
λ_a	0.760[b]	0.760[b]
λ_b	0.636[b]	0.636[b]
λ_c	0.133[b]	0.133[b]
I_a (a.m.u. Å^2)	38.6867[c]	38.6867[c]
I_b (a.m.u. Å^2)	153.959[c]	153.959[c]
I_c (a.m.u. Å^2)	170.792[c]	170.792[c]
ϱ_a $(= \lambda_a I_\alpha / I_a)$	0.06286	0.06286
ϱ_b $(= \lambda_b I_\alpha / I_b)$	0.01322	0.01322
ϱ_c $(= \lambda_c I_\alpha / I_c)$	0.002492	0.002492
ϱ $(= (\varrho_a^2 + \varrho_b^2 + \varrho_c^2)^{1/2}$	0.06429	0.06429
β $(= \arcsin[(\varrho_b^2 + \varrho_c^2)^{1/2}/\varrho])$	0.2109	0.2109
θ $(= 2\pi\,\varrho/3)$	0.1346	—
r $(= 1 - \sum_g \lambda_g^2\, I_\alpha / I_g)$	0.9435	0.9435
F $(= \hbar^2/2rI_\alpha)$ (GHz)	167.391	167.391
a_1	-2.93×10^{-6}	1.257×10^{-4}
s $(= 4V_3/9F)$	84.0 ± 1.0[d]	88.15 ± 0.08[d]
Δ_0 $(= -(3/2)\,F a_1)$ (MHz)	0.7367	−31.57
V_3 (kcal/mol)	3.02 ± 0.04[d]	3.166 ± 0.003[d]

[a] Assumed.
[b] Calculated from molecular model.
[c] Calculated from the rotational constants for the ground state using the conversion factor 505379.1 a.m.u. Å^2 according to Cohen and Taylor [13].
[d] Overlooking systematic errors of the theoretical method.

removal of the K degeneracy by odd order terms in the Hamiltonian which arise from coupling between over-all and internal rotation. For these transitions the principal axis method breaks down and has to be replaced by a treatment based on the internal axis method (IAM). To a first approximation the splittings can be calculated from the IAM applied to a molecule consisting of two coaxial symmetric tops. According to this theory the contributions of internal rotation to the A and E levels are given by [7]

$$W_{vA} = -(2/3)\,\Delta_K\,,$$
$$W_{vE\pm} = (1/3)\,\Delta_K \pm \delta_K\,,$$

where

$$\Delta_K = \Delta_0 \cos\theta\,,$$
$$\delta_K = 3^{-1/2}\,\Delta_0 \sin\theta$$

with

$$\theta = (2\pi/3)(I_\alpha/I_z)\,K$$

and

$$\Delta_0 = -(3/2)\,F\,a_1\,,$$

where a_1 is the coefficient of the second term in the expansion of the eigenvalues of the torsional equation.

When there is a slight asymmetry present in one of the tops, the factor I_α/I_z should be replaced by the following quantity

$$\varrho = (\sum_g \varrho_g^2)^{1/2}$$

where

$$\varrho_g = \lambda_g\, I_\alpha / I_g \quad \text{i.e.} \quad \theta = 2\pi\,\varrho\,K/3\,.$$

In addition to this, the asymmetry has a damping effect on the splittings which can be expanded as a power series in the angle between the vector $\boldsymbol{\varrho}$ and the a principal axis

$$\beta = \arcsin[(\varrho_b^2 + \varrho_c^2)^{1/2}/\varrho]\,.$$

In the extended fourth order formulation of Penn and Boggs [5] Δ_K and δ_K should thus be replaced by Δ_{JK} and δ_{JK}, which are given below for reference

$$\Delta_{JK} = \Delta_0[\cos\theta - (1/2)\,\beta^2(A\cos\theta - B\sin\theta) + (1/16)\,\beta^4(C\cos\theta + D\sin\theta)]$$

and

$$\delta_{JK} = 3^{-1/2} \Delta_0 [\sin\theta - (1/2)\beta^2 \times (A \sin\theta + B \cos\theta) + (1/16)\beta^4 (C \sin\theta - D \cos\theta)]$$

where

$$A = U[1 - \cos(2\pi\varrho/3)],$$
$$B = K \sin(2\pi\varrho/3),$$
$$C = (3U^2/2 - U/3 + K^2/2) + (-2U^2 + 4U/3 - 2K^2)\cos(2\pi\varrho/3) + (U^2/2 - U + 3K^2/2)\cos(4\pi\varrho/3),$$
$$D = (-4KU + 4K/3)\sin(2\pi\varrho/3) + (2KU - K)\sin(4\pi\varrho/3)$$

and

$$U = J^2 + J - K^2 .$$

Calculation of the high K, ${}^RP$ and ${}^PR$ transitions using these formulae revealed that for $s = 80$ the splittings would not exceed 0.15 MHz, which means that they are not detectable at the resolution achieved. This is a result of the fact that the internal rotation splittings of two individual levels taking part in a transition will largely cancel each other out.

For the ${}^PR$ transitions with K values between 6 and 9 the asymmetry splittings and δ_{JK} are of comparable magnitude. If the energies of the rigid rotor levels $J_{K,J-K}$ and $J_{K,J-K+1}$ are denoted by W_+ and W_- respectively, the energies of the E levels will be given by

$$E_\pm = (1/3)\Delta_{JK} + (1/2)(W_+ + W_-) \pm (1/2)[(W_+ - W_-)^2 + 4\delta_{JK}^2]^{1/2}$$

and those of the A levels by

$$A_\pm = W_\pm - (2/3)\Delta_{JK} .$$

The mixing angle ω of the E levels is given by

$$\tan(2\omega) = 2\delta_{JK}/(W_+ - W_-) .$$

If the initial and final states of a transition are denoted by the indices i and f, respectively, we obtain the following transition probabilities

$$I(\pm \to \mp) = I(b)\cos^2(\omega_i + \omega_f) + I(c)\sin^2(\omega_i - \omega_f),$$
$$I(\pm \to \pm) = I(b)\sin^2(\omega_i + \omega_f) + I(c)\cos^2(\omega_i - \omega_f),$$

where $I(b)$ and $I(c)$ are the μ_b and μ_c rigid rotor transition intensities. Several of these intermediate ${}^PR$ transitions showed detectable splittings when measured at 9 mTorr (1.2 Pa). Table 6 shows the observed and calculated splittings for the transitions $24_6 \leftarrow 23_7$ and $27_7 \leftarrow 26_8$.

Table 6. Internal rotation splittings of intermediate-K, ${}^PR$ transitions in the ground state of 1-butene oxide.

Transition	$\nu - \nu_0$ (MHz)				Intensity[d]		
	Obs.	Calc.[a]	Calc.[b]	Calc.[c]	Obs.	Calc.[a]	Calc.[c]
$24_6 \leftarrow 23_7$ [e]							
$E(- \to +)$	7.98	8.00	8.13	8.00	17	17	18
$A(- \to +)$	7.75	7.74	7.88	7.74	22	24	25
$E(+ \to +)$	7.36	7.34	7.47	7.33	11	9	7
$E(- \to -)$	−7.30	−7.30	−7.44	−7.29	8	9	7
$A(+ \to -)$	−7.83	−7.82	−7.96	−7.82	24	24	25
$E(+ \to -)$	—	−7.96	−8.09	−7.96	—	17	18
$27_7 \leftarrow 26_8$ [e]							
$E(- \to +)$	1.61	1.63	1.66	1.63	12	11	10
$A(- \to +)$	1.21	1.23	1.27	1.23	21	24	25
$E(+ \to +)$	1.02	0.99	1.02	0.99	18	15	15
$E(- \to -)$	−0.95	−0.95	−0.98	−0.95	16	15	15
$A(+ \to -)$	−1.32	−1.32	−1.35	−1.32	20	24	25
$E(+ \to -)$	−1.58	−1.59	−1.62	−1.59	13	11	10

[a] Calculated by the method described in the text.
[b] Calculated using the general IAM program of R. C. Woods, III, in its original form [11].
[c] Calculated using the Woods program with correction for centrifugal distortion included.
[d] The intensities are given in arbitrary units, normalized to to 100.
[e] The center frequencies, ν_0, are 21792.59 and 20643.14 MHz for the $24_6 \leftarrow 23_7$ and $27_7 \leftarrow 26_8$ transitions respectively. The calculated splittings correspond to $s = 84.0$. The remaining parameters are shown in Table 5.

The reason these transitions show detectable splittings is that the mixing of the internal rotation splittings with the asymmetry splitting gives rise to different sublevel patterns for the different levels. The splittings between the levels taking part in a transition will therefore no longer cancel.

The s value calculated from the splittings in the ground state is 84.0, which corresponds to a barrier height for the methyl torsion of 3.02 kcal mol^{-1}. This value should be regarded as more reliable than that obtained from the first excited state of the methyl torsion because the influence of couplings with other vibrational modes is negligible in the ground state. The high value found for s in the first excited state of the methyl torsion may be attributable to such couplings. However, there is no direct indication for a coupling between this state and the first excited heavy atom torsional state, the lines of which show no sign of splitting or even detectable increased broadening when compared with the ground state transitions. Finally, the excitation energies of the first and second excited heavy atom torsional states were calculated to be 102 cm^{-1} and 206 cm^{-1}, respectively, based on their relative intensities.

The Hamiltonian of a molecule with a symmetric internal rotor can be written in the following form

$$H = H_{\mathrm{rr}} + H_{\mathrm{ir}} ,$$

where H_{rr} represents the usual rotational energy of a rigid rotor and H_{ir}, the internal rotation contribution, has the form

$$H_{\mathrm{ir}} = (1/2\,r\,I_\alpha)(p - \varrho\,P_\varrho)^2 + V(\alpha)$$

with $P_\varrho = \boldsymbol{\rho} \cdot \boldsymbol{P}$. H_{rr} is most easily evaluated in the principal axis system in the symmetric rotor basis $|JKM\rangle$, while H_{ir} is most easily evaluated in a coordinate system where the z axis coincides with the vector $\boldsymbol{\rho}$. P_ϱ will then be diagonal in the corresponding symmetric rotor basis $|JK_\varrho M\rangle$. The transition between the two bases is, of course, effected by the irreducible representation matrices of the rotation group in the following manner (cf. [11]):

$$|JKM\rangle = \sum_{K_\varrho} |JK_\varrho M\rangle\, D^{(J)*}_{K_\varrho K}(\alpha\,\beta\,\gamma) ,$$

where α, β, and γ are the Euler angles describing the orientation of the principal axis system in the $\boldsymbol{\rho}$ coordinate system. In the approximate treatment only the diagonal elements of H_{ir} in the principal axis system are retained. They have the following form

$$\langle JKM\,v\,\sigma|\,H_{\mathrm{ir}}\,|JKM\,v\,\sigma\rangle = \sum_{K_\varrho} |\,d^{(J)}_{K_\varrho K}(\beta)\,|^2\, E_{K_\varrho v\sigma} ,$$

where β is the angle between $\boldsymbol{\rho}$ and the a principal axis. As is well known,

$$D^{(J)}_{K_\varrho K}(\alpha\,\beta\,\gamma) = \exp\{-i\,\alpha\,K_\varrho\}\, d^{(J)}_{K_\varrho K}(\beta) \exp\{-i\,\gamma\,K\}$$

whence

$$|\,D^{(J)}_{K_\varrho K}(\alpha\,\beta\,\gamma)\,|^2 = |\,d^{(J)}_{K_\varrho K}(\beta)\,|^2 .$$

For small values of β this function may be approximated by a power series in β, as was done above. Another approximation is inherent in the assumption that the internal rotation perturbations to the levels of a slightly asymmetric rotor will be the same as the corresponding diagonal elements of H_{ir} in the symmetric rotor basis. As pointed out above, this approximation breaks down in the case where the asymmetry splitting is of the same order of magnitude as δ_{JK}. In this case a Wang transformation of the symmetric rotor basis will cause the part of $(H_{\mathrm{ir}})_{KK}$ which is of odd order in K to appear off-diagonal, which will necessitate the diagonalization of a 2×2 matrix as was described above. This is, of course, still an approximation since the true asymmetric rotor functions cannot be expressed as simple Wang functions. In spite of these shortcomings the described procedure is expected to yield approximately correct values for the internal rotation splittings for a near symmetric rotor at high K values. Nevertheless, in the case of cyclopropyl methyl ether Penn and Boggs [5] found a less than satisfactory agreement between theory and experimental values for K values higher than 16.

In the general IAM program of Woods [11] the full representation matrices $D^{(J)}_{K_\varrho K}(\alpha\beta\gamma)$ are used for the basis change and the internal rotation perturbation terms are evaluated in the true asymmetric rotor basis. The only remaining approximations are thus the assumption of a high barrier and the use of perturbation theory (degenerate perturbation theory where necessary) rather than diagonalizing the complete Hamiltonian to calculate the internal rotation contributions. Although the Woods method represents a greater computational effort than the simple method described above, the requirement for manual labour is negligible. In addition, the Woods method

offers the convenience of being able to calculate the internal rotation splittings of all kinds of transitions in a single program, in contrast to the methods used above. Table 4 lists the internal rotation splittings of the first excited state of 1-butene oxide as calculated both by the PAM [10] and by the Woods program [11].

In Table 6 the internal rotation splittings of two intermediate-K, ^PR transitions with asymmetry splittings of magnitude comparable to the δ_{JK} are listed. An attempt to calculate these splittings using the original Woods program gave the correct order of magnitude but not complete agreement (Column b). Since it was inferred that this discrepancy was due to the fact that the original Woods program does not take the centrifugal distortion into consideration, which results in false values for the asymmetry splittings, the program was augmented by adding the Watson reduced Hamiltonian [10] to H_{rr} in the principal axis system to include the centrifugal distortion corrections to the same order of magnitude, as has already been described in connection with the treatment of the unsplit lines. (A similar augmentation of the Woods program has been described by Bauder and Günthard [12].) The results of the calculations with the augmented program show almost complete agreement with the experimental results (Table 6, Column c). However, the splittings observed in 1-butene oxide are too small to permit a critical comparison of the different computational methods. Also, admittedly, in its present form the Woods program does not calculate P-branch transitions, but this could be easily remedied.

Dipole Moment

The richness of the spectrum made it difficult to find suitable lines for Stark effect determinations. The best lines were the $5_{14} \leftarrow 5_{05}$ transition at 12586.35 MHz and $6_{15} \leftarrow 6_{06}$ at 13761.22 MHz, both of which exhibited pure second-order Stark shifts for fields up to 1000 V cm^{-1}. Unfortunately, these lines were found to be insensitive to the a component of the dipole moment. In order to determine this component the Stark shifts of the $6_{25} \leftarrow 6_{16}$ line at 33278.93 MHz and $5_{24} \leftarrow 5_{15}$ at 32283.98 MHz were measured. For these transitions deviations from second-order theory arise from coupling between the nearby levels 5_{24} and 5_{23} and between 6_{25} and 6_{24}, respectively. In both cases the coupling is achieved by the a component of the dipole moment operator, which makes the Stark shifts of these lines highly sensitive to μ_a.

Calculation of both the second and the mixed order Stark shifts was performed by the method described by Golden and Wilson [17] and the matrix elements of $\boldsymbol{E} \cdot \boldsymbol{\mu}$ were calculated according to the method described by Schwendeman [18] using a computer program written by M. Ribeaud of the Swiss Federal Institut of Technology for calculating the necessary coefficients for the degenerate Stark effect. In this case $\Delta\nu_M/E^2$ is no longer independent of E (for fixed M) but depends slightly on E, as seen in Table 7.

The dipole moment components were determined by a least squares fit to the measured lobes. The results of the determinations are listed in Table 7.

Table 7. Stark coefficients and dipole moment of 1-butene oxide.

Second order Stark coefficients

Transition	$\lvert M\rvert$	$10^6 \times \Delta\nu/E^2$ (MHz V^{-2} cm^2)		
		obs.	calc.	obs.-calc.
$5_{14} \leftarrow 5_{05}$	2	11.58	11.47	0.11
	3	19.21	19.40	−0.19
	4	30.74	30.50	0.24
	5	44.53	44.78	−0.25
$6_{15} \leftarrow 6_{06}$	2	5.35	5.26	0.09
	3	10.43	10.51	−0.08
	4	17.85	17.86	−0.01
	5	27.20	27.30	−0.10
	6	39.10	38.85	0.25

Mixed order Stark effect

Transition	$\lvert M\rvert$	E (V cm^{-1})	$10^6 \times \Delta\nu/E^2$ (MHz V^{-2} cm^2)		
			obs.	calc.	obs.-calc.
$6_{25} \leftarrow 6_{16}$	4	1612.5	−5.30	−5.41	0.11
	4	1814.0	−5.38	−5.40	0.02
	5	1410.9	−3.44	−3.44	0.00
	5	1612.5	−3.47	−3.43	−0.04
	5	1814.0	−3.42	−3.42	0.00
	5	2015.6	−3.35	−3.40	0.00
	6	1410.9	−1.01	−1.02	0.01
	6	1612.5	−0.962	−0.995	0.033
	6	1814.0	−0.927	−0.970	0.043
	6	2015.6	−0.864	−0.943	0.079
$5_{24} \leftarrow 5_{15}$	4	806.2	−5.82	−5.67	−0.15
	5	806.2	−8.02	−7.94	−0.08
	5	1007.8	−7.68	−7.76	0.08

$\mu_a = 0.35(2) \pm 0.004$ D, $\mu_c = 0.43(7) \pm 0.010$ D,
$\mu_b = 1.80(6) \pm 0.003$ D, $\mu_{\mathrm{tot}} = 1.89(1) \pm 0.011$ D.

The guide spacing of the Stark cell was calibrated using the $J = 2 \leftarrow 1$, $\Delta M = 0$ transition at 24325.92 MHz in the vibrational ground state of the normal species of OCS with $\mu = 0.71521$ Debye units [19].

Molecular Structure

Figure 5 shows the rotational constants calculated for 1-butene oxide as a function of the dihedral angle, θ, defined in Figure 4. These calculations were based on the assumed structural parameters of Table 8 obtained from structurally similar molecules, e.g. ethylene oxide and propylene oxide.

Of the three possible rotamers, the one corresponding to $\theta = 180°$ is unlikely to exist simply for steric reasons and calculated values for the rotational constants of this rotamer are completely different from the observed ones. Of the two remaining conformations with $\theta = 60°$ and $-60°$, calculations for the one with the methyl group

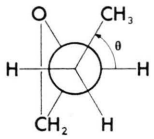

Fig. 4. Newman projection of the only observed rotamer of 1-butene oxide.

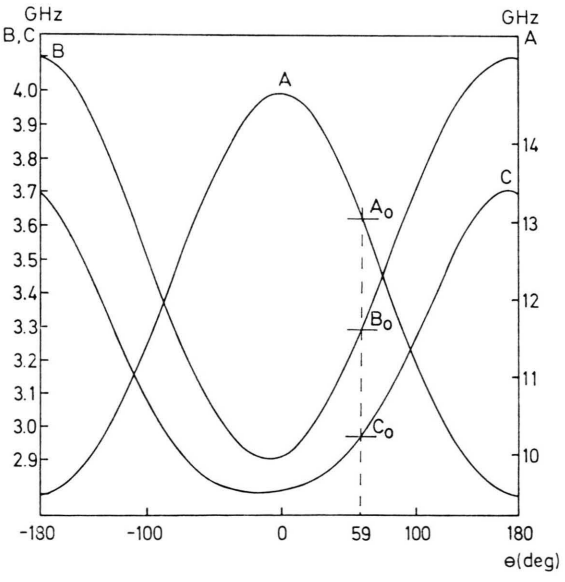

Fig. 5. Calculated rotational constants of 1-butene oxide as functions of the dihedral angle, θ, defined in Figure 4. A_0, B_0, and C_0 denote the observed spectroscopic rotational constants.

Table 8. Structural parameters for 1-butene oxide.

Assumed structural parameters [a]			
C–O	1.436 Å	∠ C_1OC_2	61.67°
C_1–C_2	1.472 Å	∠ HC_1H = ∠ HC_2C_3	116.68°
C_1–H=C_2–H	1.082 Å	∠ $C_1C_2C_3$	119.43° [b]
C_2–C_3	1.513 Å [b]	∠ HC_3H	109.43°
C_3–C_4	1.537 Å [c]	∠ HC_4H	109.43°
C_3–H	1.09 Å [c]	∠ $C_2C_3C_4$	116.68° [c]
C_4–H	1.09 Å [c]	∠ $H_2C_1C_2$ = ∠ $(HC_3)C_2C_1$ (dihedral) [d]	159.4°

Fitted structural parameter
∠ (HC_2)–(C_3C_4) (dihedral) = 59° ± 1° (θ in Figure 4)
Rotational constants (MHz)

	observed	calculated	difference
A	13063.3939	13093.223	0.2%
B	3282.5470	3273.268	0.3%
C	2959.0365	2966.672	0.3%

[a] Unless otherwise noted the assumed structural parameters were taken from reference [14].
[b] Reference [15].
[c] Reference [16].
[d] H_2C_1 and $(HC_3)C_2$ denote the bisectors of ∠ HC_1H and ∠ HC_2C_3, respectively.

closest to the oxygen atom give very good agreement (to within 0.3%) with the observed constants at $\theta = 59° \pm 1°$, while calculations for the rotamer with $\theta = -60°$ give widely different values of θ when fitting to the different rotational constants and a best root mean square deviation from the observed rotational constants of approximately 2%.

The strongest evidence that the observed spectrum derives from the rotamer with $\theta = 59°$ is, however, furnished by the dipole moment. A rather rough calculation for $\theta = 59°$ based on the assumption that the whole dipole moment of the molecule is due to the ethylene oxide fragment and neglecting other contributions yields

$$|\mu_a| : |\mu_b| : |\mu_c| = 0.084 : 1.792 : 0.562 .$$

In view of the crudeness of the model this is in acceptable agreement with the values obtained from the Stark coefficients. In contrast, a corresponding calculation for the rotamer with $\theta = -60°$ gives $|\mu_a| : |\mu_b| : |\mu_c| = 1.609 : 0.885 : 0.404$. Apart from the disagreement with the experimental values

of the dipole moment components, such a large value of μ_a would give rise to strong a-type transitions in the spectrum, contrary to the observations.

No evidence for the simultaneous existence of another rotamer was found. However, in view of the large number of unassigned low-intensity vibrational satellites present in the spectrum, the possibility of the presence of another rotamer at a concentration much lower than that of the main rotamer cannot be totally excluded.

[1] (a) S. Wolfe, Accounts of Chem. Res. **5**, 102 (1972). (b)N. S. Zefirov, Tetrahedron **33**, 3193 (1977). (c) N. D. Epiotis, J. Amer. Chem. Soc. **95**, 3087 (1973). (d) R. C. Bingham, J. Amer. Chem. Soc. **98**, 535 (1976). (e) J. E. Eilers and A. Liberles, J. Amer. Chem. Soc. **97**, 4183 (1975).
[2] R. G. Azrak and E. B. Wilson, jr., J. Chem. Phys. **52**, 5299 (1970).
[3] E. L. Eliel, N. L. Allinger, S. J. Angyal, and G. A. Morrison, Conformational Analysis, Interscience, New York, 1965.
[4] E. L. Eliel, Accounts of Chem. Res. **3**, 1 (1970).
[5] R. E. Penn and J. E. Boggs, J. Chem. Phys. **59**, 4208 (1973).
[6] S. C. Dass, A. Bhaumik, W. V. F. Brooks, and R. M. Lees, J. Mol. Spectroscopy **38**, 281 (1971).
[7] D. R. Herschbach and J. D. Swalen, J. Chem. Phys. **29**, 761 (1958).
[8] J. K. G. Watson, J. Chem. Phys. **46**, 1935 (1967).
[9] G. Steenbeckeliers and J. Bellet, J. Mol. Spectroscopy **45**, 10 (1973).
[10] D. R. Herschbach, J. Chem. Phys. **31**, 91 (1959).
[11] R. C. Woods, III, J. Mol. Spectroscopy **21**, 4 (1966).
[12] A. Bauder and Hs. H. Günthard, J. Mol. Spectroscopy **60**, 290 (1976).
[13] E. R. Cohen and B. N. Taylor, J. Phys. Chem. Ref. Data **2**, 663 (1973).
[14] G. L. Cunningham, A. W. Boyd, R. J. Myers, W. D. Gwinn, and W. I. Le Van, J. Chem. Phys. **19**, 676 (1951).
[15] J. D. Swalen and D. R. Herschbach, J. Chem. Phys. **27**, 100 (1957).
[16] Tables of Interatomic Distances and Configuration in Molecules and Ions, Chemical Society Special Publication No. 11, London, 1958.
[17] S. Golden and E. B. Wilson, jr., J. Chem. Phys. **16**, 669 (1948).
[18] R. H. Schwendeman, J. Mol. Spectroscopy **7**, 280 (1961).
[19] J. S. Muenter, J. Chem. Phys. **48**, 4544 (1968).